Computational Materials Science 79 (2013) 82–86

Contents lists available at SciVerse ScienceDirect

Computational Materials Science

journal homepage: www.elsevier.com/locate/commatsci

Electronic features induced by Stone–Wales defects in zigzag and chiral carbon nanotubes

P. Partovi-Azar [a,*], S. Panahian Jand [b], A. Namiranian [a,b], H. Rafii-Tabar [a,c]

[a] Computational Physical Sciences Research Laboratory, School of Nano-Science, Institute for Research in Fundamental Sciences (IPM), Tehran, Iran
[b] Department of Physics, Iran University of Science and Technology, Narmak, 16345 Tehran, Iran
[c] Department of Medical Physics and Biomedical Engineering, and Research Center for Medical Nanotechnology and Tissue Engineering, Shahid Beheshti University of Medical Sciences, Evin, Tehran, Iran

ARTICLE INFO

Article history:
Received 23 April 2013
Received in revised form 25 May 2013
Accepted 27 May 2013
Available online 3 July 2013

Keywords:
Carbon nanotubes
Zigzag
Chiral
Stone–Wales defect
Density-functional theory

ABSTRACT

It has been recently shown [P. Partovi-Azar, A. Namiranian, J. Phys.: Condens. Matter, 24 (2012) 035301.] that Stone–Wales (SW) defects induce different electronic features when they are formed with different angels with respect to the axis of armchair carbon nanotubes. However, the electronic features introduced by SW defects in metallic zigzag and chiral carbon nanotubes is less considered in the literature. In this paper, by means of density functional calculations, we study the electronic effects induced by SW defects in metallic zigzag and chiral tubes. We inspect how these effects change with defect orientation and concentration. We show that two and three distinctive orientations of SW defects, respectively in the case of zigzag and chiral tubes, unlike those in armchair ones, behave the same and both introduce a semiconducting gap and an electron-rich region around the defects. For zigzag tubes, the longitudinal defects open wider band gaps than circumferential ones. The value of the gaps in zigzag and chiral tubes are attributed to the degree of deformation caused by the defects.

1. Introduction

Carbon nanotubes (CNTs) have attracted numerous researchers since their discovery in 1991 [1]. The intrinsic properties of CNTs, such as thermal and electrical conductivity, make them potentially useful for production of next generation materials. Besides, possible effects of different disorders and defects in CNTs are the subject of countless investigations worldwide. Similar to other materials, physical properties of CNTs are affected by the presence of disorders. One of the most prevalent topological defects in CNTs are Stone–Wales (SW) defects which have attracted large interest from scientific community [2]. A SW defect can be imagined as a 90° rotation of single carbon bond in the hexagonal network of atoms on the surface of the tube. It is also very common in other graphitic structures like graphene [3,4]. This new orientation transforms four adjacent hexagons into two heptagons and two pentagons. This kind of defect can be introduced into the system, e.g. by single-electron irradiation [5], or by exerting stress and tension on CNTs [6]. Presence of SW defects changes the mechanical and electronic properties of CNTs [7–12]. For example, it has been predicted that the presence of SW defects on an ideal metallic CNT can make it semiconducting [13]. Moreover, it has been shown that the defective semiconducting samples with specific defect concentration can show metallic properties as well [14]. In the case of armchair, (n, n), and zigzag, $(n, 0)$, tubes, with integer n, there are two distinct orientations of SW defects. However, in the case of chiral tubes, (n_1, n_2), there are three. STM and TEM techniques [15,16], as well as some new proposed imaging methods based on the calculation of correction to the conductance of a metallic tube [17,18], which should be $G = 4e^2/h$ in otherwise perfect samples, can be used for imaging the orientation of SW defects. Some researchers have already studied the SW defects and their effects on infinitely long semiconducting zigzag [19] and on finite armchair CNTs [20,21]. However, the effects of SW defects on metallic zigzag tubes have been less studied. The literature is rather scarce in the case of chiral tubes with SW defects. This is partly due to the well-known fact that short-diameter metallic zigzag tubes $(n,0)$, with n being an integer multiple of number three, show a tiny gap [22]. Therefore, in order to investigate the band gap effects beyond it one needs to consider tubes with rather large n index. We found that for n index larger than 12, the band gap in perfect samples becomes strictly zero. Large number of atoms in a translational period (unit cell) of these structures makes first-principles

* Corresponding author. Current address: Institute of Physical Chemistry and Center for Computational Sciences, Johannes Gutenberg University Mainz, Staudinger Weg 7, D-55128 Mainz, Germany.
E-mail addresses: p.partovi@nano.ipm.ac.ir, partovia@uni-mainz.de (P. Partovi-Azar).

0927-0256/$ - see front matter © 2013 Elsevier B.V. All rights reserved.
http://dx.doi.org/10.1016/j.commatsci.2013.05.050

calculations prohibitive. This problem has been overcome to a great extent in the present work, by using finite-range orbitals as basis functions for expanding the Hamiltonian and the overlap matrices. Confined orbitals have been used in various density functional theory (DFT) codes like SIESTA [23], with already promising performance and accuracy on extensive simulations on carbon-based nanostructures, e.g. graphene [24], and even on large biological molecules and membranes [24–29].

This paper is organized as follows: in Section 2, we outline the computational method that we have used. Results are presented in Section 3 and the related discussions follow afterwards. Finally, we summarize our results and present our concluding remarks in Section 4.

2. Method of calculation

We have used the Kohn–Sham DFT [30] to find relaxed atomic coordinates and unit cell vectors of (15, 0), (6, 3) and (9, 3) tubes. The same calculations were repeated for two and three different defect orientations in zigzag and chiral tubes, respectively. We have benefited from finite-range pseudo-atomic orbitals implemented in the SIESTA density functional code [23], which allowed our computations to be efficiently performed. We have used a Troullier–Martins pseudopotential [31] for carbon with a double-ζ, singly polarized orbitals for the basis set, along with a $1 \times 1 \times 18$ Monkhorst–Pack grid [32] in the reciprocal lattice for both conformal relaxation and electronic structure calculations. We have used a real-space grid as fine as one mesh point in 4.5×10^{-4} Å^3 for describing the charge density, $\rho(\vec{r})$. We have also employed periodic boundary conditions along the tube, z-axis. The generalized gradient approximation (GGA) has been used for the exchange–correlation energy functional, E_{XC}, which, in principle, should work better than local density approximation (LDA) for systems with considerable electronic density variations. We have also used Perdew–Burke–Ernzerhof parametrization, which usually gives good results for carbon-based structures in comparison with experimental data [33]. A variable-cell relaxation has been performed on all perfect and defected CNTs until the maximum force acting on the atoms and the maximum stress tensor element fell below 0.01 eV/Å and 0.25 GPa, respectively. The target pressure has been set to 0.0 GPa. In order to calculate the local charge density of carbon π-orbitals, we considered the projected density of states, $g^{(i,m)}(\epsilon)$, in which m and i refer to the orbital and the atom, respectively. Contribution of this orbital to the total CD of the system can be obtained by integrating $g^{(i,m)}(\epsilon)f(\epsilon)$ over energies from $-\infty$ to E_F, $f(\epsilon)$ being the Fermi–Dirac distribution function [13,24]. Having finite-range atomic orbitals as basis functions enables one to calculate the hopping energies rather easily. The hopping amplitude from the orbital m of the atom i to the orbital n of the atom j, $\langle i, m|H| j, n\rangle (i \neq j)$, is the Hamiltonian matrix element $H_{im,\,jn}$. Here, we just considered the hopping between the π-orbitals of neighboring atoms.

3. Results and discussion

3.1. Metallic zigzag tubes

The defect concentration is defined here as $C_{SW} = 1/N$, where N is the number of carbon atoms in the unit cell. Fig. 1 shows the relaxed atomic configuration in the unit cells of two (15, 0) tubes with type I (a) and type II (b) SW defects, with $N = 300$, $C_{SW} \approx 0.34\%$. In the relaxed atomic configuration, there is a similarity between type I defects in zigzag tubes and type II defects reported in Ref. [13]: the diameter of the tube elongates in the vicinity of the defect. Type II defects here are also similar to type I defects in armchair tubes for the atoms near the defect tend towards the axis of the tube. The lengths of the specified bonds in Fig. 1a and b are shown in Table. 1 of the Supplementary material [34].

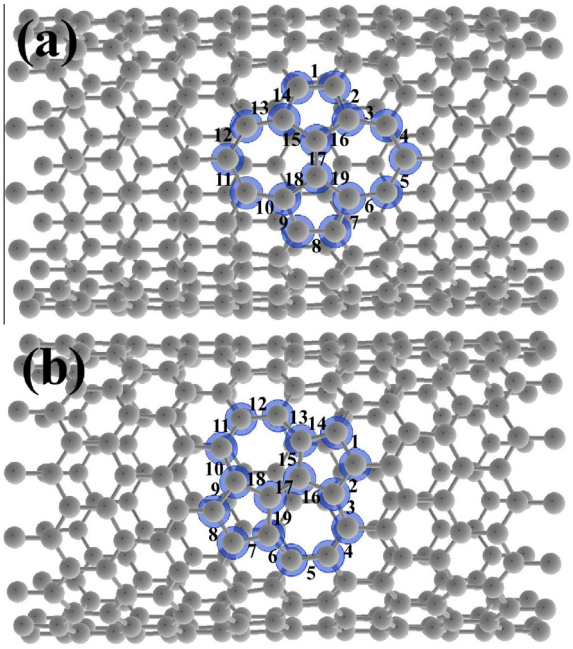

Fig. 1. Relaxed atomic configuration of the two types of SW defects on (15, 0) zigzag tubes with 300 carbon atoms per unit cell, $C_{SW} \approx 0.34\%$. (a) Shows SW defect type I, and (b) shows type II.

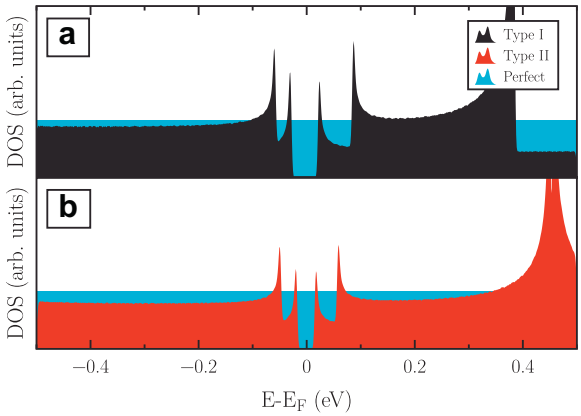

Fig. 2. Electronic density of states (DOS) near the fermi energy for a (15, 0) tube with (a) type I and (b) type II SW defect. The blue histogram is the DOS for a perfect sample, plotted for comparison.

Fig. 2 shows electronic density of states (DOS) near the Fermi energy, E_F, for a perfect (15, 0) sample, a (15, 0) sample with type I defect, and a (15, 0) sample with type II defect, with same defect concentration. It is necessary to mention here that the band gaps are usually underestimated within DFT [36]. Therefore, here we mostly focus on qualitative band gap effects induced by SW defects. The histogram in blue is the DOS for a perfect sample. Unlike SW defects in armchair tubes [13], here both types of SW defects open a small band gap near E_F irrespective of their orientation. This is also reflected in the local charge density (CD) distribution of π-orbitals around two types of defects shown Fig. 1 in the Supplementary material [34]. Type I and type II defects on zigzag tubes form electron-rich regions around them. This is in contrast to the CD distribution near SW defects in armchair tubes [13], where